



**AFRL-AFOSR-VA-TR-2022-0117**

---

**Study of HV Dielectrics for High Frequency Operation in Linear and Nonlinear Transmission Lines and Simulation and Development of Hybrid Nonlinear Lines for RF Generation**

**Rossi, Jose**  
**FUNCATE - FUNDACAO DE CIENCIAS**  
**CONTRACTS OFFICE**  
**SAO JOSE DOS CAMPOSSP, , 12210131**  
**BR**

---

**02/25/2022**  
**Final Technical Report**

**DISTRIBUTION A: Distribution approved for public release.**

Air Force Research Laboratory  
Air Force Office of Scientific Research  
Arlington, Virginia 22203  
Air Force Materiel Command

## REPORT DOCUMENTATION PAGE

PLEASE DO NOT RETURN YOUR FORM TO THE ABOVE ORGANIZATION.

<b>1. REPORT DATE</b> 20220225	<b>2. REPORT TYPE</b> Final	<b>3. DATES COVERED</b>	
		<b>START DATE</b> 20171215	<b>END DATE</b> 20201214
<b>4. TITLE AND SUBTITLE</b> Study of HV Dielectrics for High Frequency Operation in Linear and Nonlinear Transmission Lines and Simulation and Development of Hybrid Nonlinear Lines for RF Generation			
<b>5a. CONTRACT NUMBER</b>		<b>5b. GRANT NUMBER</b> FA9550-18-1-0111	<b>5c. PROGRAM ELEMENT NUMBER</b>
<b>5d. PROJECT NUMBER</b>		<b>5e. TASK NUMBER</b>	<b>5f. WORK UNIT NUMBER</b>
<b>6. AUTHOR(S)</b> Jose Rossi			
<b>7. PERFORMING ORGANIZATION NAME(S) AND ADDRESS(ES)</b> FUNCATE - FUNDACAO DE CIENCIAS CONTRACTS OFFICE SAO JOSE DOS CAMPOSSP 12210131 BR			<b>8. PERFORMING ORGANIZATION REPORT NUMBER</b>
<b>9. SPONSORING/MONITORING AGENCY NAME(S) AND ADDRESS(ES)</b> Air Force Office of Scientific Research 875 N. Randolph St. Room 3112 Arlington, VA 22203		<b>10. SPONSOR/MONITOR'S ACRONYM(S)</b> AFRL/AFOSR IOS	<b>11. SPONSOR/MONITOR'S REPORT NUMBER(S)</b> AFRL-AFOSR-VA-TR-2022-0117
<b>12. DISTRIBUTION/AVAILABILITY STATEMENT</b> A Distribution Unlimited: PB Public Release			
<b>13. SUPPLEMENTARY NOTES</b>			
<b>14. ABSTRACT</b> This report describes the main results obtained in the research project on special solid-state devices, known as Nonlinear Transmission Lines (NLTLs) and used in RF generation, in the period from Dec./2017 to Dec./2020. We studied two types of NLTLs for aerospace applications: discrete LC with variable capacitors and continuous coaxial lines (gyromagnetic) with ferrite cores. In the first case, discrete lines were designed from LT-SPICE simulations and built with silicon carbide Schottky diodes (SiC) for operation around 200 MHz at high voltage (700 V). In this case, the irradiation tests were made in an anechoic chamber for EMI suppression with emitting and receiving DRG antennas. With gyromagnetic lines, emphasis was on developing a prototype for operation in the 3 to 5 kV range, using Ferroxcube ferrites with an outer diameter of 9 mm and an exponential input pulse generator from FID Technologies with a pulse width of 10 ns.			
<b>15. SUBJECT TERMS</b>			
<b>16. SECURITY CLASSIFICATION OF:</b>		<b>17. LIMITATION OF ABSTRACT</b>	<b>18. NUMBER OF PAGES</b>
<b>a. REPORT</b> U	<b>b. ABSTRACT</b> U	<b>c. THIS PAGE</b> U	SAR 16
<b>19a. NAME OF RESPONSIBLE PERSON</b> GEOFFREY ANDERSEN			<b>19b. PHONE NUMBER (Include area code)</b>

## **AFSOR Final Performance Report**

**Title:** Study of HV Dielectrics for High Frequency Operation in Linear and Nonlinear Transmission Lines and Simulation and Development of Hybrid Nonlinear lines for RF Generation

**Grant/ Contract Number:** FA9550-18-1-0111

**Start Date:** 15 Dec. 2017

**Manager:** Dr. Geoffrey Andersen  
AFOSR/IO  
875 North Randolph St.  
Arlington VA, 22203  
(703) 615-9465  
geoffrey.andersen.4@us.af.mil

**PI:** Dr. Jose O. Rossi  
National Institute for Space Research  
1758 Astronautas Ave.  
Sao Jose dos Campos, SP, Brazil, 12227-010  
+ 55 (12) 3208 6695  
jose.rossi@inpe.br

## I. ABSTRACT

This report describes the main results obtained in the research project on special solid-state devices, known as Nonlinear Transmission Lines (NLTLs) and used in RF generation, in the period from Dec./2017 to Dec./2020. We studied two types of NLTLs for aerospace applications: discrete LC with variable capacitors and continuous coaxial lines (gyromagnetic) with ferrite cores. In the first case, discrete lines were designed from LT-SPICE simulations and built with silicon carbide Schottky diodes (SiC) for operation around 200 MHz at high voltage (700 V). In this case, the irradiation tests were made in an anechoic chamber for EMI suppression with emitting and receiving DRG antennas. With gyromagnetic lines, emphasis was on developing a prototype for operation in the 3 to 5 kV range, using Ferroxcube ferrites with an outer diameter of 9 mm and an exponential input pulse generator from FID Technologies with a pulse width of 10 ns.

## II. INTRODUCTION

This report keeps focusing on the analysis and operation of nonlinear transmission lines (NLTLs) used in high-power RF or microwave generators for applications in vehicles and mobile platforms, replacing the use of electronic tubes such as magnetrons, TWTs, etc. [1-3]. The advantage of NLTLs is their compact and simple construction since they do not need auxiliary voltage and filament sources like tubes. They can be of two types: discrete or continuous. In the case of discrete NLTLs, the device consists of a network composed of capacitors or inductors, where both [4, 5] or at least one of the components (L or C) is nonlinear [6]. The nonlinearity, in this case, is characterized by the decrease of  $C(V)$  or  $L(I)$  with the voltage and current, respectively. Fig. 1 shows an intermediate section of a capacitive NLTL composed of two variable capacitors.

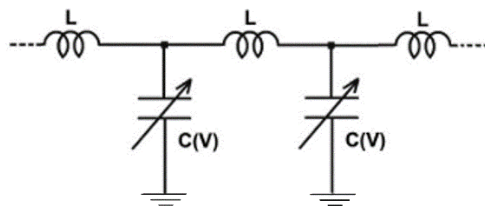


**Fig. 1.** Schematic of an intermediate section of a capacitive NLTL.

As the nonlinear discrete line is also dispersive, for the RF generation, the pulse injected at the input of the line needs to have a rise time lower than the inverse of the cutoff frequency of the line (given by  $f_c = 1/\pi\sqrt{LC(V)}$ ), as shown in Fig. 2. The cutoff line frequency also limits the RF frequency band generated. Besides,

as soon as the pulse propagates along the line, the pulse amplitude top travels faster than its base because the propagation velocity increases with the nonlinear line capacitance  $C(V)$  decrease, producing pulse sharpening at the output [7-9]. The counterpart of the  $C(V)$  line using nonlinear inductance  $L(I)$  generates the same effects.

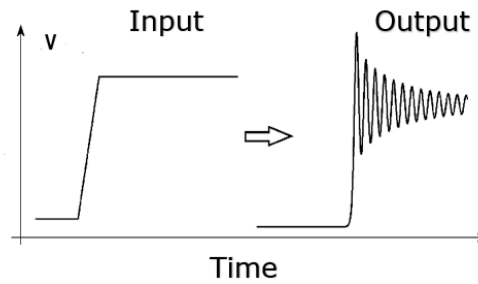


**Fig. 2.** RF generation process in a discrete line.

For the case of continuous NLTLs, known as gyromagnetic [10-15], the RF generation principle is a little different, as they operate immersed in an axial field  $H_z$  produced by a solenoid wound on the outer conductor of the line, as shown in Fig. 3. In this way, as the high voltage pulse feeds the line, the azimuthal field generated by the pulse current around the conductor displaces the ferrite magnetic domains initially aligned with axial magnetic bias, causing the precession movement of magnetic dipoles. The phenomenon of magnetic field precession can be described with accuracy by the Landau-Lifshitz-Gilbert (LLG) equation in the LL form as:

$$\frac{\partial \mathbf{M}}{\partial t} = \frac{\gamma}{1+\alpha^2} [-\mathbf{M} \times \mathbf{H}_{eff} - \frac{\alpha}{M_s} \mathbf{M} \times (\mathbf{M} \times \mathbf{H}_{eff})], \quad (1)$$

where  $\mathbf{M}$  is the ferrite magnetization vector,  $\mathbf{H}_{eff}$  the resultant effective magnetic field vector,  $M_s$  the saturated ferrite magnetization,  $\gamma = 1.76 \times 10^{11} \text{ rad.s}^{-1}.\text{T}^{-1}$  the gyromagnetic ratio of the electron and  $\alpha$  the precession damping constant that depends on the material. The precession frequency of the total magnetic field depends on the axial magnetic field, input voltage, load, and properties of the magnetic medium. Ferrite's high-frequency precession induces high-frequency oscillations in the pulse as it propagates along the line. The resulting pulse waveform at the output is like the input pulse but with a reduced rise time due to line nonlinearity and a series of RF oscillations superimposed on the pulse amplitude. Unlike discrete LC lines in which the Bragg frequency limits pulse rise time, in the case of gyromagnetic lines, the nonlinear properties of the magnetic material limit the pulse sharpening.

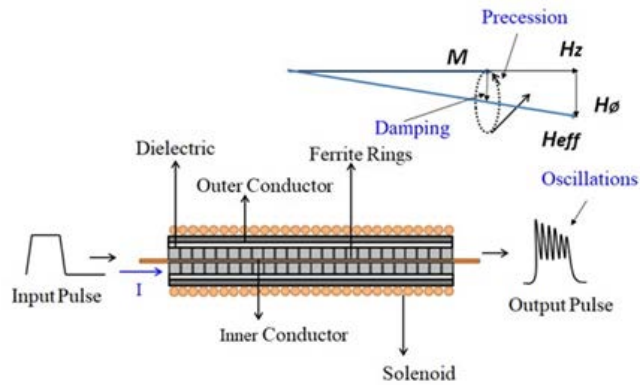


**Fig. 3.** Schematic of a gyromagnetic line showing the dynamics of RF generation.

### III. PROPOSED GOALS

In the research project, two goals were proposed for the period:

- a) To demonstrate the operation of a discrete capacitive NLTL at high frequencies up to 200 MHz at high voltage, using Schottky SiC diodes with a reverse voltage of 1 kV and inductors with cores of air in the nH range.
- b) To build a short 20-cm gyromagnetic line as a prototype and validate the results using numerical modeling for the line.

### IV. RESULTS OBTAINED

This section presents the main results obtained for each of the goals proposed during the period of the project:

#### A. Discrete capacitive NLTL

The discrete capacitive NLTL implemented using a printed circuit board (PCB) with 12 sections is shown in Fig. 4, and with linear air-core inductors of 56 nH and SiC Schottky diodes, model C4D02120E, as nonlinear elements [16].

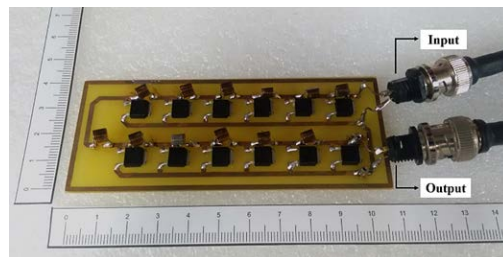


**Fig. 4.** Capacitive discrete line mounted with SiC diodes and linear inductors.

We used the LT-SPICE XVII program as the circuit modeling software. The simulated circuit consists of 12 concentrated LC sections, as shown in Fig. 5, with fixed 56-nH inductors. The variable varactor diode capacitance and the corresponding QxV curves from the datasheet and modeling are in Fig. 6(a) and (b) but made with adjustments in the capacitance values as a function of the stray capacitances present in the PCB. Resistances corresponding to the ohmic losses of inductors and capacitors were added, whose values were, respectively, 0.1  $\Omega$  and 2.0  $\Omega$ . An arbitrary pulse generator supplies the line with the same characteristics to the model 9355-1 generator, applying a pulse with an amplitude of 800 V at the NLTL input, with a width of 34 ns and a rise and fall times of 1 ns. A 50- $\Omega$  impedance load placed at the line output is assumed.

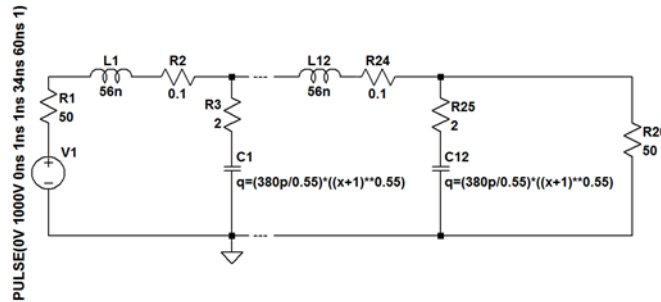


Fig. 5. Schematic of the simulated line circuit.

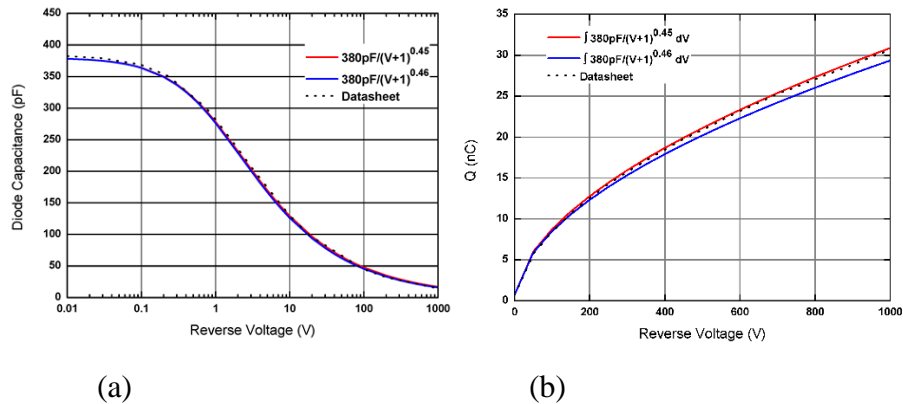
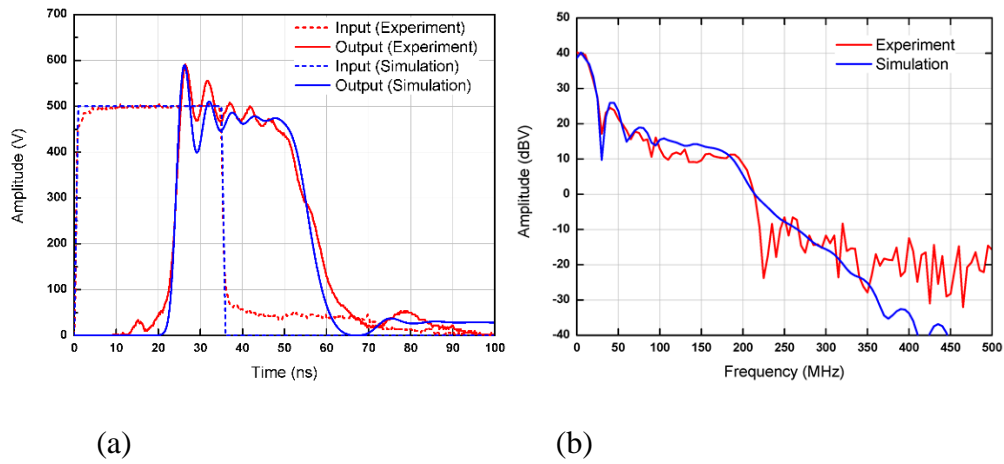


Fig. 6. Capacitance and respective charge versus the reverse voltage for C4D02120E diode.

Fig. 7 (a) and (b) show the SPICE simulations of the output and input pulses (in blue) in both the time and frequency domains, respectively, providing a good agreement with the experimental results (in red). The results demonstrate an oscillation frequency of the order of 200 MHz, a value slightly below the theoretical calculation of the line cut-off frequency,  $f_c = 1/\pi\sqrt{LC(V_{max})}$ , considering the value  $C(V_{max})$  adjusted on the order of 40 pF.



**Fig. 7.** Discrete line input/output pulses obtained in the time and frequency domain (FFT).

To extract the RF signal for radiating, this signal through an antenna a decoupling circuit was implemented at the end of NLTL, through an impedance matching circuit, removing the DC component of the output signal generated by the NLTL, as shown in the setup used by the block diagram in Fig. 8.



**Fig. 8.** Block diagram of the setup implemented for the irradiation tests.

The irradiation tests used a pyramidal transmitting horn antenna connected to the NLTL output and a receiving pyramidal horn antenna, separated by a 2-m distance. Figure 9 shows the experimental setup used for the irradiation tests inside a shielded anechoic chamber [17].

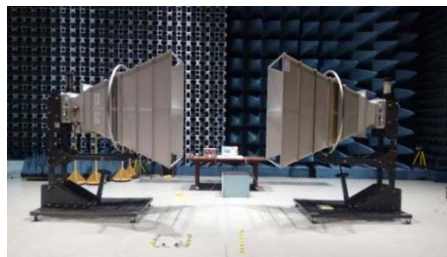


**Fig. 9.** Experimental setup implemented for irradiation tests.

The uncoupled signal injected into the input of the transmit antenna is seen in Fig. 10(a) with the respective waveform simulated, and the signal received by the receiving antenna in Fig. 10(b).

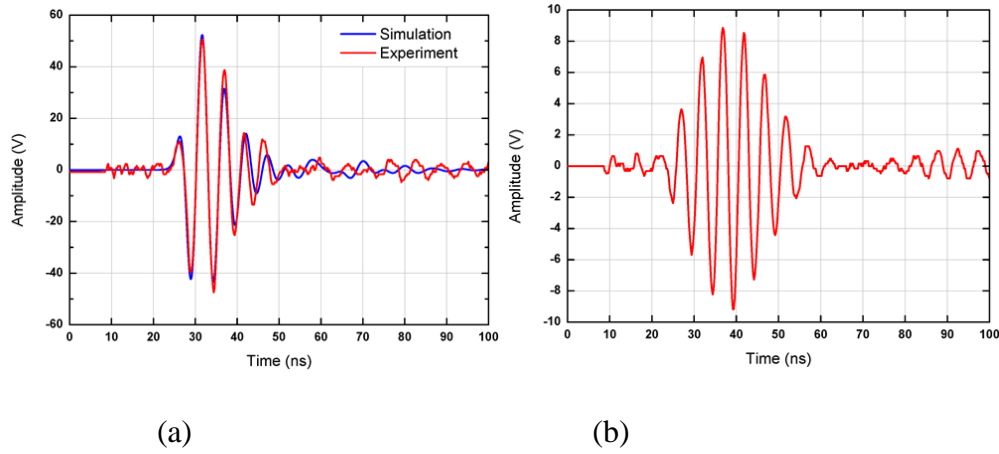


**Fig. 10.** Decoupled signal on transmission (left) and signal received on reception (right).

The results obtained in the irradiation tests, around 200 MHz, confirm the frequency generated at the line output as shown by the FFT in Fig. 11.

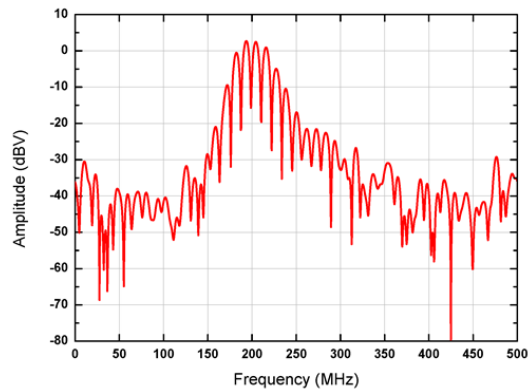


**Fig. 11.** FFT of the signal measured at the receiving antenna with a peak near 200 MHz.

## B. Gyromagnetic NLTLs

A first experimental prototype was built and tested using a solenoid to produce the axial field initially [18-20] to study and evaluate the performance of the gyromagnetic NLTL. The MiZn ferrite cores used were from Ferroxcube (see Fig. 12), model TN9/6/3 with external and internal diameters of about 9 and 6 mm, respectively. The ferrite magnetic permeability given in the datasheet is of the order of 800. We removed a 20-cm length of the insulation layer and the outer braiding of a coaxial cable to place 60 ferrite Ferroxcube rings. Two layers of Kapton wrapped around the ferrites isolate rings and keep the structure rigid. A copper tape wrapped around the insulating layer of the ferrite rings work as ground. The ends of the line were terminated with coaxial connectors to connect the generator to the 50-ohm attenuators in a safe way to avoid electromagnetic interference.



**Fig. 12.** The ferrite cores from Ferroxcube used and the gyromagnetic line built.

The test system (Fig. 13) consists of a 5 kV/20 ns high-voltage pulse generator from FID- Technologies to supply the gyromagnetic line with a fast pulse with a rise time of the order of 2 ns and exponential decay, plus a 30 A DC source to power the solenoid and to generate the axial magnetic field. The high-voltage requirement is to produce a high azimuthal magnetic field inside the ferrites. A coil built with 1860 turns of AWG13 copper wire ( $\phi = 1.828$  mm) in 5 layers on 80-cm length of a metallic tube with a diameter of 20 cm needs a current of around 11.0 A to generate 30.0 kA/m for the axial magnetic field polarization. Two high-voltage attenuators from Solar Electronics, placed between the output of the coaxial line and the input of the Agilent Technologies 2.5 GHz digital oscilloscope (model DSO9104A), keep the oscilloscope input voltage below 5.0 V. The attenuators used have the following specifications: 2500-V peak, 40-dB attenuation, and 2.5-W average power. As the permeability of ferrite depends on the pulse current amplitude, the line impedance changes with time. Thus, the line impedance calculation is not precise because the line impedance varies during pulse application, but the estimation of the saturated line impedance is possible. Dividing the saturated line inductance of 148.0 nH/m by the linear capacitance of the line estimated at 75.0 pF/m gives a value of 44.0 ohms approximately.

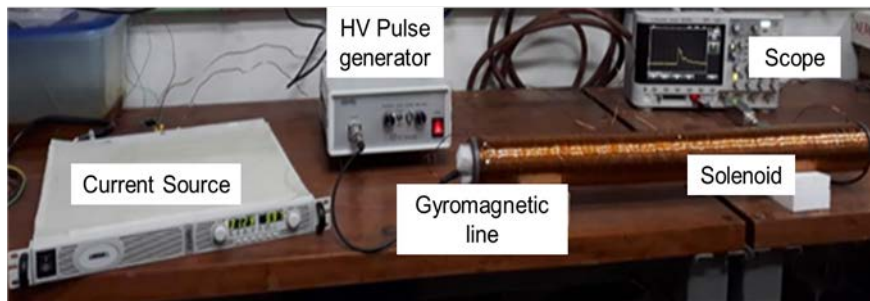


**Fig. 13.** The experimental set-up employed to test the gyromagnetic line prototype [18].

The first results of the 20 cm long gyromagnetic line (GNLTL) performed in operation with high output voltage pulses of the order of 2-3 kV are presented in Fig. 14 to verify the influence of the magnetic field on the device performance. The GNTL introduced into the solenoid was subjected to the external axial field  $H_z$  with the DC source turned on to power the solenoid. A current of 11.0 A through solenoid corresponded to an intensity  $H_z = 30$  kA/m. First, the measurement considered the signal extracted at the output without magnetic field applied (in black in Fig. 14) and compared it with the output signal with  $H_z$ -field (in blue in Fig 14).

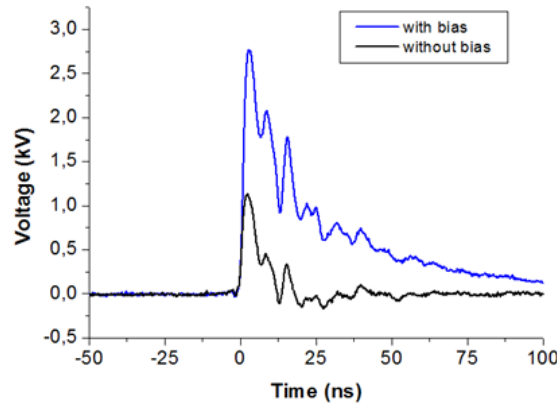


**Fig. 14.** GNLTL output signals with and without H-field bias applied.

With the two signals compared in Fig. 14, note the pulse amplitude under the axial field  $H_z$  is approximately three times greater than the case without the field. The explanation for this is that under the influence of the magnetic field, the line impedance is close to 50 ohms, keeping matched to the pulse generator impedance, 50-ohm scope input, and RF attenuators. Thus, the pulse emerges at the output of the line with a higher amplitude peak with axial  $H_z$ -field bias. Furthermore, more oscillations with greater depth of voltage modulation are generated under axial magnetic polarization due to the strong alignment of the ferrite electron spins before pulse application. Fig. 15 shows the corresponding fast Fourier transform (FFT) measured through the digital oscilloscope of the pulses shown in Fig. 14, with and without a magnetic field. As shown in Fig. 15, when the GNLTL is under the influence of the magnetic field, the FFT provides a very sharp peak frequency located in the range close to 180 MHz compared to the non-biased case. In short, the comparison between the two signals (with and without a magnetic field) proves the influence of the axial field on the performance of the line, related to oscillations and voltage modulation amplitudes shown in Fig. 14. With Fig. 15, the peak frequency of the FFT is more evident with greater amplitude with axial magnetic polarization.

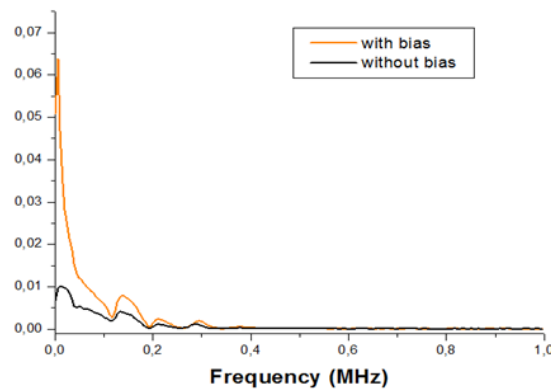


**Fig. 15.** FFTs of the output signals shown in Fig. 14.

The experimental results with magnetic field configuration have been compared with simulations using SPICE circuit software and a numerical method known as finite differences in the time domain-FDTD [21]. Initially, it was made modeling in LT-SPICE, where the continuous gyromagnetic line was considered as a discrete LC line of several sections and the gyromagnetic effect represented by variable inductors with magnetic flux given by a hyperbolic tangent function. However, this modeling was not producing satisfactory results compatible with the experiment data and therefore only the results of the FDTD model were considered. In summary, the FDTD method, as in SPICE for the simulation, considers the continuous gyromagnetic line formed by a series of sections, but in this case, the equations were spatially discretized in the LC cells in elements of length  $\Delta x$ , represented in Fig. 16, where  $V_s$  represents the generator voltage,  $R_s$  the generator resistance and  $R_L$  the load resistance.

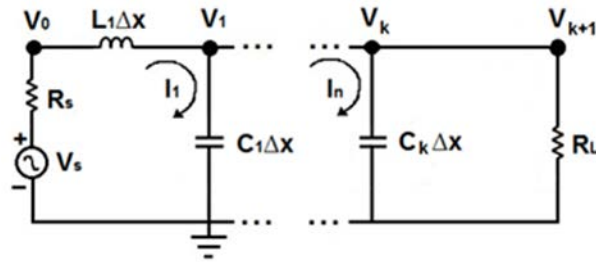


**Fig. 16.** Equivalent circuit of an LC discrete line used in the FDTD method.

In our case, the numerical simulation codes were developed using the Free Software OCTAVE, version 5.0.2. The equations below show the sequence of equations used in the numerical coding of this iteration method for the voltage and current at the node  $k$  and at a discretized time  $n$ :

$$V_k^n = V_k^{n-1} - \frac{\Delta t}{C_0 \Delta x} [I_k^n - I_{k-1}^n] \quad (2)$$

$$I_k^n = I_k^{n-1} - \frac{\Delta t}{L_0 \Delta x} [V_{k+1}^n - V_k^n] - \mu_0 \cdot \left( \frac{d_m - d_i}{2} \right) \cdot \frac{\Delta t}{L_0} \cdot \frac{dM_k^n}{dt} \quad (3)$$

where  $L_0$  and  $C_0$  are the inductance and capacitance per section,  $d_m$  and  $d_i$  are the outer and inner diameters of the ferrite ring, and  $\Delta x$ ,  $\Delta t$  are respectively space and time increments respectively. For each calculation of  $dM/dt$  at the node  $k$  and at the discretized time  $n$ , it is assumed to use the LLG equation shown in (1). Next, Fig. 17 shows the result of the FDTD simulation of the output pulse for comparison to the experimental result with the magnetic field in Fig. 14. Note that there is a reasonable agreement between experiment and simulation, in terms of peak voltage reached and sequence of oscillations, despite the greater number of oscillations with better modulation in amplitude in the simulated case, which can be explained by the fact that the losses of the ferrite and dielectric in

numerical modeling have not yet been implemented. Although the FFT of the signal was not shown, it was also verified that the RF generation remained in simulation as in the experimental case in the 180-200 MHz band.

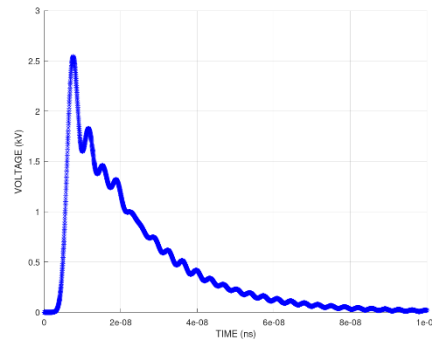


**Fig. 17.** FDTD simulation of the output pulse signal from GNLTL.

## V. CONCLUSIONS

We investigated two types of NLTL devices used for RF generation in this report: discrete and gyromagnetic lines. With the discrete lines, a significant scientific advance was made with the high-voltage RF generation at 200 MHz using silicon carbide (SiC) diodes and DRG antennas for irradiation tests for use in pulsed transmission systems. Also, the trend of this research indicates a possible reduction of the input pulse generator in compact applications and an increase in the RF band generation above 500 MHz using SiC varactor diodes. Reaching this trend is essential for compact applications in space, as weight reduction is the main requirement for use in space vehicles, and antennas in the L-band are already much smaller in size than in the VHF band. With the gyromagnetic lines, the prospect for passing the operation from 200 MHz to the L-band (1-2 GHz) is good. For this, we expect to increase the intensity of the azimuthal field with a pulse generator of higher output voltage and using a ferrite ring of small dimensions as the field strength is inversely proportional to the ferrite mean diameter. Recent simulations by the FDTD method have indicated that using a generator with a capacity of 12 kV will be enough to reach 1-2 GHz. Also, the FDTD simulation method using the OCTAVE software has produced better results for GNTLs than SPICE. Moreover, for a fully compact gyromagnetic line, a solution will be the replacement of the solenoid employing permanent magnets, which suppress the need for a DC power source.

## REFERENCES

- [1] GAUDET, J.A. ET AL., "Research Issues in Developing Compact Pulsed Power for High Power Pulse Applications on Mobile Platforms," Proceedings of the IEEE, vol. 92, no. 7, July 1992, pp. 1144-1165.
- [2] GAUDET, J.A.; SCHAMILOGLU, E.; ROSSI, J.O.; BUCHENAUER, C.J.; Frost, C., "Non-Linear Transmission Lines for High Power Microwave Applications – A Survey," Proc. of the 2008 IEEE IPMHVC, Las Vegas, NV, May 2008, pp. 131-138.

- [3] SMITH, P.W. Transient Electronics, West Sussex, England: John Wiley & Sons, 2002.
- [4] ROSSI, J.O.; RIZZO, P. N., "Study of Hybrid Nonlinear Transmission Lines for High Power RF Generation," Proceedings of the 2009 IEEE Int. PPC, Washington, DC, June 2009, pp. 46-50.
- [5] KUEK, N. S.; LIEW, A. C.; SCHAMILOGLU, E.; ROSSI, J. O., "RF pulse generator based on a nonlinear hybrid line." IEEE Transaction on Plasma Science, vol. 42, no. 10, pp. 3268-3273, Oct. 2014.
- [6] KUEK, N. S.; LIEW, A.C.; SCHAMILOGLU, E.; ROSSI, J. O., "Pulsed RF oscillations on a nonlinear capacitive transmission line." IEEE Transaction on Dielectric and Electrical Insulation, vol. 20, no. 4, pp. 1129-1135, Aug. 2013.
- [7] WILSON, C.R.; TURNER, M.M.; SMITH, P.W., "Pulse Sharpening in a Uniform LC Ladder Containing Nonlinear Ferroelectric Capacitors" IEEE Transactions on Electron Devices, vol. 38, no. 4, pp. 767-771, 1991.
- [8] BAKER, R.J. ET AL., "Generation of kV-Sub Nanosecond Pulses Using a Nonlinear Line," Meas. Sci. Technol. 4 (1993) 893-985.
- [9] IBUKA, S. ET AL., "Fast High Voltage Pulse Generator with Nonlinear Transmission Line for High Repetitive Operation," in Proc. of the 1995 IEEE Int. PPC, pp. 1365-1370.
- [10] SULLIVAN III, W.; DICKENS, J.; KRISTIANSEN, M., "Shock Wave Simulation of Ferrite Filled Coaxial Nonlinear Transmission Lines," in Proc. of the 2008 IEEE IPMHVC, Las Vegas, NV, May 2008, pp. 517-520.
- [11] CHADWICK, S.J.F; SEDDON, N.; RUKIN, S., "A Novel Solid-State HPM Source Based on a Gyromagnetic NLTL and SOS-Based Pulse Generator," in Proc. of the 18th IEEE Int. PPC, Chicago, IL, June 2011, pp. 178-181.
- [12] BRAGG, J.; DICKENS, J.; NEUBER, A., "Temperature Dependence on Ferrimagnetic Based Nonlinear Transmission Line," in Proc. of the 18th IEEE Int. PPC, Chicago, IL, June 2011, pp. 182-184.
- [13] ROMANCHENKO, I.V. ET AL., "Repetitive Sub-Gigawatt RF Source Based on Gyromagnetic Nonlinear Transmission Line," Review of Scientific Instruments 83, 074705 (2012).
- [14] AHN, J.W.; KARELIN, S.Y.; KWON, H.O.; MAGDA, I.I.; SINITSIN, V.G., "Exciting high frequency oscillations in a coaxial transmission line with a magnetized ferrite," Journal of Magnetism, v. 20, n. 4, p. 460-465, 2015.
- [15] KARELIN, S. Y.; KRASOVITSKY, V. B.; MAGDA, I. I.; MUKHIN, V. S.; SINITSIN, V. G., "Radio frequency oscillations in gyrotropic nonlinear transmission lines", In *Plasma*, 2, 258-271, 2019.
- [16] RAIMUNDI, L. R.; ROSSI, J. O.; RANGEL, E. G. L.; SILVA, L. C.; SCHAMILOGLU, E., "High-voltage capacitive nonlinear transmission lines for RF generation based on silicon carbide Schottky diodes," IEEE Transactions on Plasma Science, v. 40, n. 1, p. 566-573, 2019.
- [17] ROSSI, J. O.; SILVA, L. C.; RAIMUNDI, L. R.; RANGEL, E. G. L.; SCHAMILOGLU, E., "Pulsed RF signal irradiation using a low voltage NLTL coupled to a DRG antenna," In: IEEE Pulsed Power and Plasma Science Conference, Orlando, June 2019.
- [18] YAMASAKI, F. S.; ROSSI, J. O.; RANGEL, E. G. L.; SCHAMILOGLU, E.; SILVA, L. C., "Operation of a gyromagnetic line with magnetic axial bias," in: IEEE Pulsed Power and Plasma Science Conference, Orlando, June 2019.
- [19] DOLAN, J.E.; BOLTON, H.R., "Shock front development in ferrite-loaded coaxial lines with axial bias," IEE Science, Measurement and Technology, vol. 147, no. 5, pp.237-242, Sept. 2000.
- [20] YAMASAKI, F.S; ROSSI, J.O.; BARROSO, J.J.; SCHAMILOGU, E., "Operation of a gyromagnetic line at low and high voltages with simultaneous axial and azimuthal biases," IEEE Transactions on Plasma Science, v. 46, n. 7, p. 2573-2581, July 2018.
- [21] A. F. G. Greco, J. O. Rossi, F. S. Yamasaki, J. J. Barroso, E. Schamiloglu and L. P. da Silva Neto, "1D-FDTD Simulation of Microwave Generation Using Ferrite Electromagnetic Shock Lines," 2020 IEEE Electrical Insulation Conference (EIC), 2020, pp. 344-347, doi: 10.1109/EIC47619.2020.9158728.

## Publications acknowledging AFOSR support result from this grant

### A) Periodicals

- 1) F. S. Yamasaki, J. O. Rossi, J. J. Barroso and E. Schamiloglu, "Operation of a Gyromagnetic Line at Low and High Voltages With Simultaneous Axial and Azimuthal Biases," in *IEEE Transactions on Plasma Science*, vol. 46, no. 7, pp. 2573-2581, July 2018, doi: 10.1109/TPS.2018.2840425
- 2) L. P. Silva Neto, J. O. Rossi, J. J. Barroso and E. Schamiloglu, "Hybrid Nonlinear Transmission Lines Used for RF Soliton Generation," in *IEEE Transactions on Plasma Science*, vol. 46, no. 10, pp. 3648-3652, Oct. 2018, doi: 10.1109/TPS.2018.2864214.
- 3) L.C. Silva, J.O. Rossi, E.G.L Rangel, L.R Raimundi and E. Schamiloglu, "Study of pulsed RF signal extraction and irradiation from a capacitive nonlinear transmission line," in *Int. Journal of Advanced Engineering Research and Science*, v. 5, n. 10, p. 121-133, Oct. 2018., doi: 10.22161/ijaers.5.10.17.
- 4) L. R. Raimundi, J. O. Rossi, E. G. L. Rangel, L. C. Silva and E. Schamiloglu, "High-Voltage Capacitive Nonlinear Transmission Lines for RF Generation Based on Silicon Carbide Schottky Diodes," in *IEEE Transactions on Plasma Science*, vol. 47, no. 1, pp. 566-573, Jan. 2019, doi: 10.1109/TPS.2018.2873491.
- 5) E. G. L. Rangel, J. O. Rossi, J. J. Barroso, F. S. Yamasaki and E. Schamiloglu, "Practical Constraints on Nonlinear Transmission Lines for RF Generation," in *IEEE Transactions on Plasma Science*, vol. 47, no. 1, pp. 1000-1016, Jan. 2019, doi: 10.1109/TPS.2018.2876020.

### B) Conference Proceedings

- 1) J. O. Rossi, F. S. Yamasaki, E. Schamiloglu and J. J. Barroso, "Analysis of nonlinear gyromagnetic line operation using LLG equation," *2017 IEEE 21st International Conference on Pulsed Power (PPC)*, 2017, pp. 1-3, doi: 10.1109/PPC.2017.8291172.
- 2) J. O. Rossi, E. G. L. Rangel, L. P. S. Neto and E. Schamiloglu, "Study of the Nonlinear Phenomena in Ceramic Dielectric Composite Used in Compact PFLs," *2018 IEEE International Power Modulator and High Voltage Conference (IPMHVC)*, 2018, pp. 288-290, doi: 10.1109/IPMHVC.2018.8936753.
- 3) L. P. Silva Neto, J. O. Rossi, J. J. Barroso, E. G. L. Rangel and E. Schamiloglu, "Improving the voltage modulation depth and RF power generated on Nonlinear Transmission lines," *2018 IEEE International Power Modulator and High Voltage Conference (IPMHVC)*, 2018, pp. 416-420, doi: 10.1109/IPMHVC.2018.8936795.

- 4) L. C. Silva, J. O. Rossi, L. R. Raimundi, E. G. L. Rangel and E. Schamiloglu, "Analysis of Pulsed RF Signals Radiated from a Capacitive NLTL," 2018 IEEE International Power Modulator and High Voltage Conference (IPMHVC), 2018, pp. 461-463, doi: 10.1109/IPMHVC.2018.8936843.
- 5) L. R. Raimundi, J. O. Rossi, E. G. L. Rangel, L. C. Silva, E. Schamiloglu and L. P. S. Neto, "RF Generation at 200 MHz Using a SiC Schottky Diode Lumped NLTL," 2018 IEEE International Power Modulator and High Voltage Conference (IPMHVC), 2018, pp. 473-476, doi: 10.1109/IPMHVC.2018.8936827.
- 6) E. G. L. Rangel, J. O. Rossi, J. J. Barroso, L. P. S. Neto and E. Schamiloglu, "Dielectric and Magnetic Nonlinear Materials for NLTLs," 2018 IEEE International Power Modulator and High Voltage Conference (IPMHVC), 2018, pp. 269-273, doi: 10.1109/IPMHVC.2018.8936831.
- 7) E. G. L. Rangel et al., "The Development of Capacitive Nonlinear Transmission Lines and Its Performance Limits," 2019 IEEE Pulsed Power & Plasma Science (PPPS), 2019, pp. 1-4, doi: 10.1109/PPPS34859.2019.9009883.
- 8) L. P. Silva Neto, H. M. Moraes, J. O. Rossi, J. J. Barroso, E. Rangel and A. F. Conceição, "Development of an RF circuit amplifier fed by a low power nonlinear transmission line," 2019 IEEE Pulsed Power & Plasma Science (PPPS), 2019, pp. 1-4, doi: 10.1109/PPPS34859.2019.9009881.
- 9) F. S. Yamasaki, J. O. Rossi, L. C. Silva, E. G. L. Rangel and E. Schamiloglu, "Operation of a Gyromagnetic Line with Magnetic Axial Bias," 2019 IEEE Pulsed Power & Plasma Science (PPPS), 2019, pp. 1-4, doi: 10.1109/PPPS34859.2019.9009907.
- 10) L. C. Silva, J. O. Rossi, L. R. Raimundi, E. G. L. Rangel and E. Schamiloglu, "Pulsed RF Signal Irradiation Using a Low Voltage NLTL Coupled to a DRG Antenna," 2019 IEEE Pulsed Power & Plasma Science (PPPS), 2019, pp. 1-4, doi: 10.1109/PPPS34859.2019.9009627.
- 11) A. F. G. Greco, J. O. Rossi, F. S. Yamasaki, J. J. Barroso, E. Schamiloglu and L. P. da Silva Neto, "1D-FDTD Simulation of Microwave Generation Using Ferrite Electromagnetic Shock Lines," 2020 IEEE Electrical Insulation Conference (EIC), 2020, pp. 344-347, doi: 10.1109/EIC47619.2020.9158728.
- 12) J. O. Rossi, E.G.L. Rangel, F.S. Yamasaki, A.F.G. Greco, A.F. Teixeira, J.J. Barroso, L.P. Silva Neto, E. Schamiloglu, "Research status on nonlinear transmission lines for RF generation," presented at the 47th IEEE International Conference on Plasma Science (ICOPS-2020) and 2nd ASIA Pacific Conference on Plasma and Terahertz Science (APCOPTS-2020). (Virtual Event).

## **Collaborations on the subject supported by this grant**

- Dr. Edl Schamiloglu – University of New Mexico- Dept. of Electrical and Computer Engineering - Head of Pulsed Power, Beams and Microwave Laboratory, NM, USA.

- Dr. Lauro Paulo da Silva Neto – Federal University of Sao Paulo- ICT- Sao Jose dos Campos-SP- Brazil.

## **Interactions**

### **A) Conference Participation/Workshop/Lecture**

- Dr. Jose O. Rossi – Power Modulator and HV Conference (IPMHVC)- Jackson Lake Lodge, WY, USA, June 2018.
- Dr. Jose O. Rossi – Pulsed Power and Plasma Science (PPPS) – Orlando, FL, USA, June 2019.
- Dr. Jose O. Rossi – Plasma and Electro-energetic Physics Portfolio Energetic Review –Virtual Event, June 2020.
- Dr. Jose O. Rossi – Electrical Insulation Conference (EIC)- Virtual Event, June 2020.
- Dr. Jose O. Rossi – International Conference on Plasma Science (ICOPS)- Virtual Event, Dec. 2020.

### **B) Technical Visits supported by this grant**

- Dr. Edl Schamiloglu- National Institute for Space Research -Sao Jose dos Campos, SP, Brazil, Aug. 2018.
- Dr. Edl Schamiloglu- National Institute for Space Research -Sao Jose dos Campos, SP, Brazil, Aug. 2019.

## **Personnel**

- Edl Schamiloglu -CO-PI- Professor at ECE/UNM- USA
- Lauro Paulo da Silva Neto- Professor at ICT/UNIFESP- BRAZIL
- Dr. Fernanda S. Yamasaki – Pos-doc
- Ana Flavia Guedes Greco – Grad Student
- Elizete Gonçalves Lopes Rangel – Scientist Staff
- Joaquim José Barroso- Retired Scientist Staff
- André Ferreira Teixeira – Grad Student